# Feasibility of Active Debris Removal Testing on the International Space Station using Free-flyers

Vaios Lappas[*]
*Department of Mechanical Engineering and Aeronautics, University of Patras, Greece*

Antonios Tsourdos[†]
*Cranfield University, Cranfield, Bedfordshire, MK43 0AL, United Kingdom*

Thomas Peters[‡]
*GMV, Madrid, Spain*

Hanspeter Schaub[§]
*University of Colorado, Boulder, Colorado, 80309-0429, USA*

Robin Biesbroek[**]
*European Space Agency, Netherlands*

## Abstract

Various Active Debris Removal (ADR) mission concepts and technologies are currently being developed in which the objective is to capture and remove large space debris from orbit [2-17]. The use of a tethered system for de-orbiting by pulling the target debris has shown to be promising. Tethered systems use a net or harpoon to capture the target debris, which may be tumbling with unpredictable rates. The tethered link between a chaser and debris target is also maintained and needs to be controlled in order to de-orbit the debris, where several de-orbit maneuvers are executed, Then, aerodynamic forces during atmospheric re-entry force the tether and chaser/ target) to disintegrate. Dynamics of tethered systems with 2 large end bodies is challenging, with many aspects still unexplored. The goal of this study is to use existing free-flyer infrastructure on the ISS, in order to perform realistic, low cost experiments, in a scaled fashion, based on realistic ADR mission scenarios. It is shown, through representative simulations and analysis, that free-flyer experiments on the ISS are feasible and can provide unique insight on the dynamics and design of tethered systems.

## Nomenclature

| | | |
|---|---|---|
| $A$ | = | tether cross-sectional area, $m^2$ |
| $c$ | = | tether damping constant, kg/s |
| $E$ | = | Young's modulus, GPa |
| $\boldsymbol{F}$ | = | actuation force, N |
| $\mathbf{I}$ | = | inertia tensor, $kg \cdot m^2$ |
| $k$ | = | tether spring constant, N/m |
| $\boldsymbol{L}$ | = | external known torque, Nm |
| $\boldsymbol{l}$ | = | tether link length vector, m |
| $l$ | = | tether length, m |
| $m$ | = | mass, kg |

[*]Professor in Aerospace Systems, Department of Mechanical Engineering and Aeronautics, University of Patras, Greece, vlappas@upatras.gr, Senior Member AIAA.
[†]Director of Research, School of Aerospace, Transport, Manufacturing, a.tsourdos@cranfield.ac.uk, AIAA Member.
[‡] Project Manager, Space Systems, GMV
[§] Professor, Glenn L. Murphy Endowed Chair, Aerospace Engineering Sciences, University of Colorado
[**] Systems Engineer, European Space Agency, Netherlands

$\boldsymbol{R}$ = position vector, m
$\boldsymbol{r}_{port}$ = tether attachment point location, m
$\boldsymbol{T}$ = tether tension force, N
$\boldsymbol{V}$ = velocity vector, m/s
$\Delta l$ = required tether elongation, m
$\Delta t$ = time step, s
$\mu$ = Earth's gravitational constant, $m^3/s^2$
$\boldsymbol{\omega}$ = angular rate vector, rad/s
$\omega_n$ = natural frequency, rad/s
Subscripts
$C$ = chaser
0 = initial value

## I. Introduction

Today's space debris environment poses a safety hazard to operational spacecraft, as well as a hazard to safety of persons and property in cases of uncontrolled re-entry events. Studies show that the problem will continue to grow unless a number of inactive space debris are removed every year [1-3]. Various Active Debris Removal (ADR) mission concepts and technologies are currently being developed in which the objective is to capture and remove a large space debris from orbit [2-17]. The use of a tethered system for de-orbiting by pulling the target debris has shown to be promising in a series of studies over the past three years, culminating in Europe with the European Space Agency's Cleanspace Program and the e.Deorbit ADR reference mission concept [17]. Tethered systems use a net or harpoon to capture the target debris, which may be tumbling with unpredictable rates [4-6, 8-17]. Once captured, a tethered link exists between the chaser spacecraft and the capture mechanism. This tethered link will continue to exist, when the target is de-tumbled or the tumbling motion of the debris can potentially be using thrust maneuvers. The tethered link between a chaser and debris target is also maintained and needs to be controlled in order to de-orbit the debris, where several de-orbit maneuvers are executed, each lowering the perigee of the chaser-tether-debris system to a final perigee of roughly 40 km. Then, aerodynamic forces during atmospheric re-entry force the tether (and both chaser and target) to disintegrate.

Dynamics of tethered systems with 2 large end bodies is challenging, with many aspects still unexplored. In a paper by Jasper and Schaub [10], the authors studied the tether dynamics and continuous open-loop thrust input shaping to attenuate the violent dynamics of TSS and hence avoid the collision between the end bodies. This approach, however, can be challenging due to the discrete on/off thruster capabilities. Several discrete thrust input shaping techniques are studied in [11]. These approaches are more realistic for on-off thrusters and offer better performance with respect to a step input in terms of end bodies collision avoidance and target attitude motion. The target's angular rate during tethered towing is studied in [12], however, the target's attitude has not been analyzed in detail. Investigation of the target's attitude is important in an active debris removal (ADR) mission scenario in order to avoid a tether wrapping up around the target and thus avoiding possible in-orbit collisions. The authors in [10] also emphasized the influence of the tether parameters, such as length, Young's modulus and damping ratio, on the system dynamics. Aslanov and Yudintsev [14] analyze the rotational motion of the target, when constant low thrust is applied by the active spacecraft. The study reveals that initial target orientation or initial slack in the tether can lead to tether tangling around the target which can result in tether rupture thus creating new debris in orbit. The study, however, does not consider closed-loop control of the chaser and its attitude motion impact on the target rotation. Following a deorbit burn, closed loop control of the chaser's attitude and relative position with respect to the target is analyzed in Ref [13]. Closed-loop control is advantageous due to the increased safety achieved by avoiding the collision between the end bodies and robustness for uncertain target mass and inertia properties. Nevertheless, closed-loop control adds complexity to the system, requires careful consideration of sensor performance and may increase the control effort due to sensor noise. This paper focuses on studying the feasibility of testing critical ADR maneuvers of a tethered chaser-debris target in a scaled manner, on the International Space Station, using free-flyers. Free flyers have been in operation on the ISS since 2006, specifically the MIT Synchronized Position-Hold, Engage, Reorient Experimental Satellites - SPHERES. Three SPHERES free-flyers are utilized to test many control algorithms in space (ISS), allowing for rapid and low cost prototyping and validation on complex control algorithms, such as rendezvous/docking, formation flying and guidance with machine vision [18].

The goal of this study is to use existing free-flyer infrastructure on the ISS, in order to perform realistic, low cost experiments, in a scaled fashion, based on the realistic ADR mission scenario of ESA's e.Deorbit reference study to remove a large debris target. This paper is organized as follows. In Section II, the ISS free flyer technology available

and being planned to be operated is presented. Section III gives an overview of the e.Deorbit ADR reference mission along with debris stabilization and towing maneuvers which are to be implemented as scaled experiments on the ISS. Section IV discusses the feasibility of testing critical ADR maneuvers on the ISS in a constrained volume where supporting simulations demonstrate the feasibility of such experiments. Section V provides detailed simulations of critical ADR maneuvers which can be conducted on the ISS and explain the various trade-offs in the system design of the tether (length, diameter, material) and Section VI presents the experimental set-up proposed using existing ISS infrastructure and the limited sensors and rigs needed. Finally Section VII draws the conclusions.

## II. ISS Free Flyers

### A. MIT SPHERES Free-flyer

The MIT Synchronized Position-Hold, Engage, Reorient Experimental Satellites -SPHERES- is a free flyer test bed aboard the ISS which utilizes three experimental satellites, designed for providing researchers with a long term, replenishable, and upgradeable testbed for the validation of high risk metrology, control, and autonomy technologies [18, 19]. It features the ability of easy abort-improve-repeat approaches, i.e. all experiments are observed by astronauts and can easily be aborted. After evaluating the results on ground the algorithms can be improved and tests can be repeated in a subsequent test session. Moreover, re-programming of the satellites allows for changing the control algorithms with respect to varying test objectives. The SPHERES is a high fidelity test bed designed for developing and maturing algorithms for distributed satellite system concepts. The SPHERES program began as a design course in the Space System Laboratory (SSL) at MIT and developed over the years to a permanent robotic experiment aboard the ISS [19].

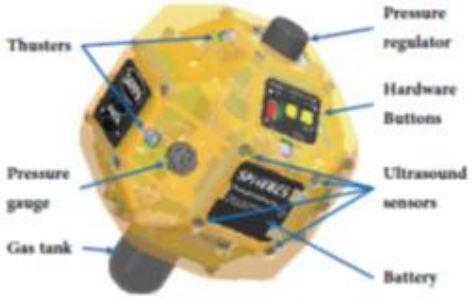


| Property | Value |
|---|---|
| **Diameter** | 0.22m |
| **Mass (with tank and batteries)** | 4.3kg |
| **Max. linear acceleration** | 0.17m/s$^2$ |
| **Max. Angular acceleration** | 3.5rad/s$^2$ |
| **Power Consumption** | 13W |
| **Battery Lifetime** | 2h |

**Figure 1: Main components (left) and basic properties (right) of a SPHERE Satellite [18, 19]**

The SPHERES spacecraft control their position and attitude using a cold gas system. Multi-phase $CO_2$ is stored in a tank located inside the satellites. It is regulated to 25 psi and fed through an expansion capacitor to the 12 valve thruster, which are distributed over the surface and controlled via pulse-width modulation. Hardware buttons on a control panel are used to power and reset the satellite, initiate the boot-loading of the test software, and enable the satellite for the tests. The basic properties of the satellites are summarized in Figure 1 (right) and Table 1. The experimental satellites feature a full 6-DoF control authority. The built-in navigation system consists of a custom pseudo-GPS based on ultrasound beacons and sensors. The beacons are located at the borders of the test volume such as the walls of the Japanese Experiment Module (JEM). This enables the SPHERES to perform absolute state measurements. Given a priori knowledge about the beacon configuration, the on-board computer performs time-of-flight measurements and additionally uses three accelerometers and three gyroscopes to estimate its state. The sensor fusion is done by an Extended Kalman Filter (EKF), reaching a precision in the vicinity of $10^{-3}$ m [19].

| Parameter | Value |
|---|---|
| **Thrusters** | 12/6 DOF |
| **Thrust** | 0.1N |
| **Minimum Firing time** | 10 ms |
| **Propellant** | CO2 860psi/35 psi regulated |
| **Spheres Diameter** | 21 cm |
| **Mass** | 4.4 kg (full CO2 Tank) |
| **Power** | AA Batteries |
| **ADCS** | Gyros, accelerometers, Ultrasound sensors |
| **OBC** | TI TMS320C6701 floating point DSP, Sundance SMT375 board |
| **FDIR** | FDI, mass ID algorithms implemented in C / Embedded C++ |

| | |
|---|---|
| **Controls** | 10 Hz control update, 1 kHz gyro sampling |
| **RF Comm's** | SPHERES-SPHERES and SPHERES-laptop |
| **Experiment Time** | Multiple ~2-hour experiment sessions enable *experimental iteration* |
| **Autonomy/Safety** | Astronaut supervised, interior to ISS |

**Table 1: SPHERES System Parameters**

SPHERES are currently used to mature space technology. Scientists on the ground and astronauts aboard the ISS, initiate, monitor, and occasionally restart the experiments as well as change consumables such as propellant tanks and batteries. In this way, SPHERES is a risk-tolerant test bed that can be used for robotic control in space. Complex tests can be performed in a representative environment under zero gravity conditions and full 6-DoF control, without the danger of losing hardware in case the test conditions prove too challenging [18]. Since its commissioning in 2006, about 28 SPHERES test sessions, each featuring approximately 10-15 tests, were executed aboard ISS. The test sessions have included research on Formation Flight [19], Docking and Rendezvous [20], Fluid Slosh, Fault Detection, Isolation, and Recovery (FDIR) [21], and general distributed satellite systems control and autonomy. Before being uploaded to ISS, the flight experiment software is integrated and verified with the SPHERES test bed on a 3-DoF (two degrees of translational and one degree of rotational freedom) air-bearing table at MIT SSL. The satellites are put on floating devices that are equipped with additional $CO_2$ tanks. Analogously to the SPHERES testing environment on ground, the equipment aboard ISS is composed of three nanosatellites, communications hardware, replenishable consumables (tanks and batteries), and an astronaut interface. Figure 2 (left) shows the complete SPHERES setup in the JEM, where SPHERES experiments are currently conducted. Previously, the U.S. Destiny Laboratory (US Lab) was used for SPHERES test sessions. The current test volume is approximately a 2 m cube (JEM Module). A complete test session (TS) usually takes between two and three hours of crew time. After a first introductory crew conference, the astronaut sets up and configures the hardware. An ISS-supplied standard laptop is used as a control station to upload new programs to the satellites, collect telemetry and interact with the experiment.

### B. NASA Ames Astrobee Free Flyer

Astrobee will be a free-flying robot that can be remotely operated by astronauts in space or by mission controllers on the ground. NASA is developing Astrobee to perform a variety of intravehicular activities (IVA), such as operations inside the International Space Station (ISS) [22]. These IVA tasks include interior environmental surveys (e.g., sound level measurement), inventory and mobile camera work. Astrobee will also serve as a platform for robotics re-search in microgravity. NASA has been developing the Astrobee free-flying robot since 2014 as part of the NASA Human Exploration Telerobotics 2 (HET2) project. This new robot will build upon technology and lessons learned from the Smart Synchronized Position Hold, Engage, Reorient, Experimental Satellite (Smart SPHERES) robot.

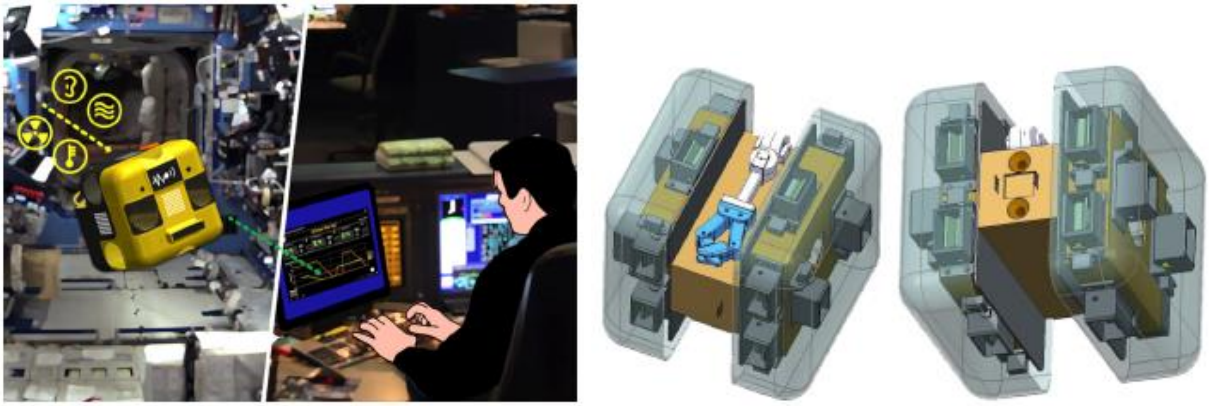

**Figure 2: Artist Concept of the Astrobee free-flying robot [22]**

Astrobee will be designed to address a variety of scenarios including mobile sensor (e.g., imagers or sound level meters), auto-mated logistics (e.g., mobile inventory), and free-flying robotic test bed. Astrobee will develop and test robot technologies required for autonomous operations, mobility, remote operation by ground controllers, and human-robot interaction with crew. These technologies include propulsion, robot user interface (proximal and remote), supervisory control, payload interface, and navigation. At the highest level, the system includes the Astrobee itself, a dock-resupply station for replenishing power, and any necessary hardware and software for communication, control and data transfer. The Astrobee will be self-contained and autonomous with the capability of being manually controlled as well. Ideally it will be capable of fully autonomous localization and navigation inside the ISS USOS.

The Astrobee will have video cameras on board allowing it to serve as a remotely operated mobile camera platform that may be used for localization and navigation. The Astrobee will also have expansion ports where additional sensors/hardware can be attached for demonstration, testing and use aboard the station. Additional sensors that may be attached to or integrated with the Astrobee include a radio-frequency identification reader and the necessary software to communicate with the inventory management system, a sound level meter, and a high-definition camera [22].

The proposed ADR tests on the ISS are designed as simple, low cost experiments which can be implemented either using the SPHERES or Astrobee free-flyers on the ISS. In this paper, we focus on using SPHERES hardware, as the hardware is currently being used for various GNC experiments on the ISS and require no modification other than simple mechanical fixtures and COTS sensors for the proposed ADR experiments which are analysed and detailed in Section V.

## III. Active Debris Removal Reference Scenario

Space Debris poses a significant problem for satellites and astronauts in orbit. With the number of space debris increasing, there is a renewed effort to develop technical solutions, methods and analyze possible techniques to capture, tow and perform controlled re-entry of space debris objects which pose the largest danger for in-orbit collisions. Many agencies, institutions are currently investigating how debris can be removed from low earth orbit (LEO). In this work, the European Space Agency e.Deorbit active debris removal (ADR) mission study is used as a reference mission, to study the attitude control implications of towing a large satellite such as Envisat using a tether. The e.Deorbit mission concept has been studied by several actors, including ESA, see [17, 23]. The objective of the e.Deorbit mission is to remove Envisat from orbit. All studies investigated several concepts for capturing the target, including robotic arms, tentacles, nets and harpoons. The nets and harpoons imply a flexible connection or tether between the chaser and the target. The tether transmits the force generated by the main thrusters on the chaser to the target in order to provide the $\Delta V$ required for de-orbiting. The most recent e.Deorbit studies need to take into account the fact that Envisat has experienced an increase in angular velocity to about 3.5 °/s [23]. This implies, that the first action the chaser must take after capture (either by harpoon or net), is to stabilize the target and reduce the angular velocity to zero. A component of the towing part of the missions which are currently being heavily analyzed is the tether. Ref [17] shows the overall configuration of Envisat, including the definition of the body fixed reference frame axis directions. The origin of the body reference frame is at the interface plane of the spacecraft interface ring. Table 2 shows the mass properties, dimensions and orbit parameters of Envisat and chaser. Figure 3b shows the baseline chaser for the work presented in this paper. The chaser has been developed by Airbus Defense and Space for ESA for the e.Deorbit program [23, 24]. Figure 3b also shows the chaser spacecraft model including the body fixed frame. The platform design is based on a platform similar to the DEOS mission. In this image, the net launch canisters are the round light orange structures placed on the raised circular platform in the center of the top face of chaser. Two net launch canisters are carried such that two capture attempts can be made. The chaser platform design is compact and has a low mass. The chaser design features 4 main engines of 425 N (two redundant engines), four intermediate, 220 N engines and twenty-four 22 N RCS engines [23, 24]. In our study only two 425 N thrusters are used.

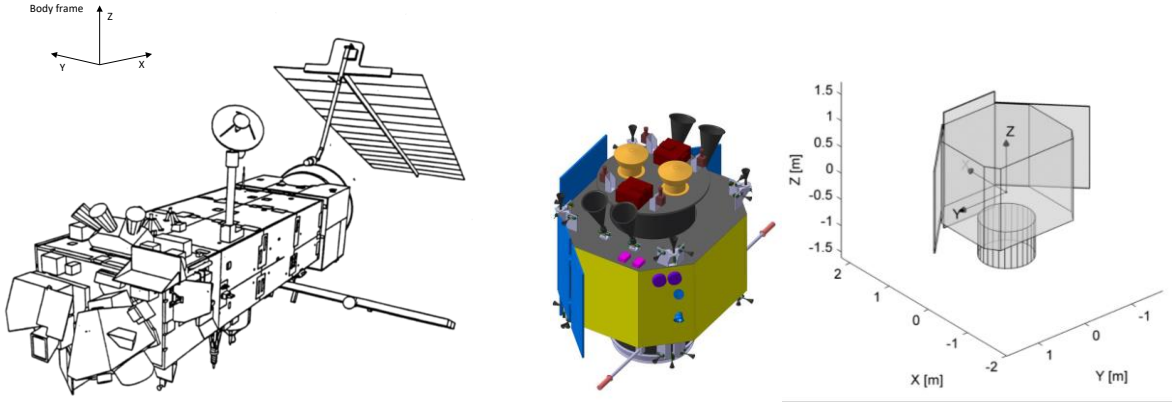


**Figure 3: (a) Envisat (b) Chaser layout and body frame**

The dynamics system considered in the paper consists of a chaser, debris and a tether connecting the two bodies, see Fig. 4. Each of the end bodies is modeled as a rigid body which can translate and rotate, resulting in a 6 degrees

of freedom model. The target is assumed to be a passive, inactive satellite, in our case ENVISAT. The chaser has an active control system which is able to deliver both pure force and torque. The tether is discretized into 2 point masses and 3 equidistant massless tether links. Each tether element is modeled as a parallel spring-damper system. It is assumed that the tether attachment points on the chaser and target are not located in the center of mass of the end bodies, but are displaced relatively to the center of mass of each body. The displacement of the tether attachment points with respect to the center of mass is described by the vectors $\boldsymbol{r}_{port,C}$ and $\boldsymbol{r}_{port,T}$, for the chaser and the target, respectively. Therefore, when the neighboring tether links connected to the end bodies are stretched, the torque is applied. It must be emphasized, that when the deployed net is considered, there will be many attachment points between the net and the target. Due to numerous contact points, the damping of the target rotational motion will likely increase [10-13]. In this paper, one tether attachment point is considered which considerably simplifies the model and can be regarded as a worst-case scenario in terms of target angular rate damping.

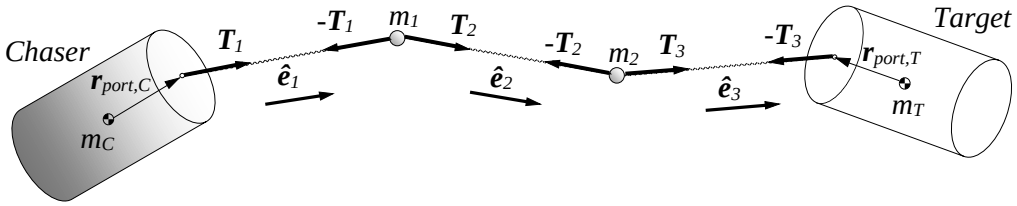


**Figure 4: Discretized tether model with 2-point masses and 3 tether elements**

| Parameter | Value |
|---|---|
| **Envisat (Debris target)** | |
| Mass [kg] | 7827.8 |
| $I_{xx}$, $I_{yy}$, $I_{zz}$ [kgm$^2$] | (17023.3, 124825.7, 129112.2) |
| $I_{xy}$, $I_{yz}$, $I_{zx}$ [kgm$^2$] | (397.1, 344.2, -2171.1) |
| CoM (x, y, z) [m] | (-3.905, -0.009, 0.003) |
| Dimensions (body) [m x m x m] | 10.02 x 2.75 x 1.6 |
| Dimensions (Solar panel) [m x m x m] | 14.028 x 4.972 x 0.01 |
| Length [m] | 26.024 |
| Eccentricity | 0.000117 |
| Inclination (°) | 98.3274 |
| Perigee height (km) | 765 |
| Apogee height (km) | 766 |
| RAAN (°) | 303.2 |
| Argument of perigee (°) | 81.03 |
| **Chaser Spacecraft** | |
| Mass [kg] | 1610 |
| $I_{xx}$, $I_{yy}$, $I_{zz}$ [kgm$^2$] | (1100, 1160, 450) |
| $I_{xy}$, $I_{yz}$, $I_{zx}$ [kgm$^2$] | (0, 0, 0) |
| Capture Method | Net |
| Main thrust (N) | 1700 |
| Perigee [km] | 70 |
| disposal $\Delta$V (ms$^{-1}$) | 190 |
| N burns | 3 |

**Table 2: Envisat and Chaser Properties [23, 24]**

The attitude dynamics of each end body is given by the Euler equation:

$$\dot{\boldsymbol{\omega}} = \mathbf{I}^{-1}\left(\boldsymbol{M} + \boldsymbol{M}_{gg} + \boldsymbol{r}_{port} \times \xi \boldsymbol{T} - \boldsymbol{\omega} \times \mathbf{I}\boldsymbol{\omega}\right) \tag{1}$$

where all vectors are expressed in body frame. The first term in the parenthesis on the right-hand side of Eq. (1), $\boldsymbol{M}$, denotes the actuation torque, $\boldsymbol{M}_{gg}$ corresponds to the gravity gradient torque, third term denotes the torque generated by the neighboring tether link force and the last term is the gyroscopic term. Note, that for the passive target, the actuation torque is $\boldsymbol{M} = 0$.

### A. ADR Mission Scenario Overview

The analyzed ADR scenario begins with the target and the chaser in a circular orbit with an altitude of 800 km. It is assumed that the chaser has performed successful rendezvous and target capture [17, 23]. The chaser is located behind the target and along the orbital in-track direction. Three scenarios are investigated: (i) Stabilization after capture (ii) De-orbit burn (plus stabilization) (iii) Stabilization during atmospheric pass

*1. Stabilization after capture*

The initial rotation rate of the target is 5 °/s around the body y-axis, which is aligned with the y-axis of the LVLH frame. The length of the tether is 50 m and it has a 4100 kN/m stiffness. The frequency of the on-board software (OBSW) used is 5 Hz, along with four 220N thrusters ESA e.Deorbit reference ADR study [17, 23]. During the initial stabilization phase the assist thrusters are used to ensure that the attitude motion of the target can be stopped. The assist thrusters are active during the first 700 seconds after capture. Figure 5shows a typical simulation image of the stabilization scenario. The tether is shown in blue, with mass points represented as dots. The chaser trajectory is shown in red (zoomed in frame - Fig. 5). In this particular simulation, the chaser moves along a small ‘figure 8’ trajectory. In this nominal stabilization case, all thrusters are used (220N and 22N RCS thrusters).

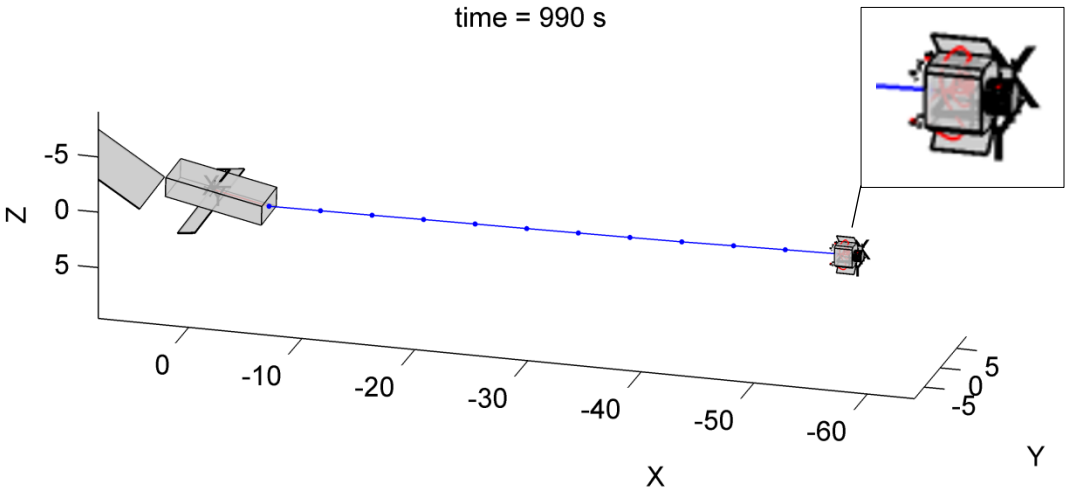


**Figure 5: Simulation of ADR stabilization scenario**

Figure 6a shows the tension in the tether. The tension remains well below the maximum tension allowed for Dyneema.

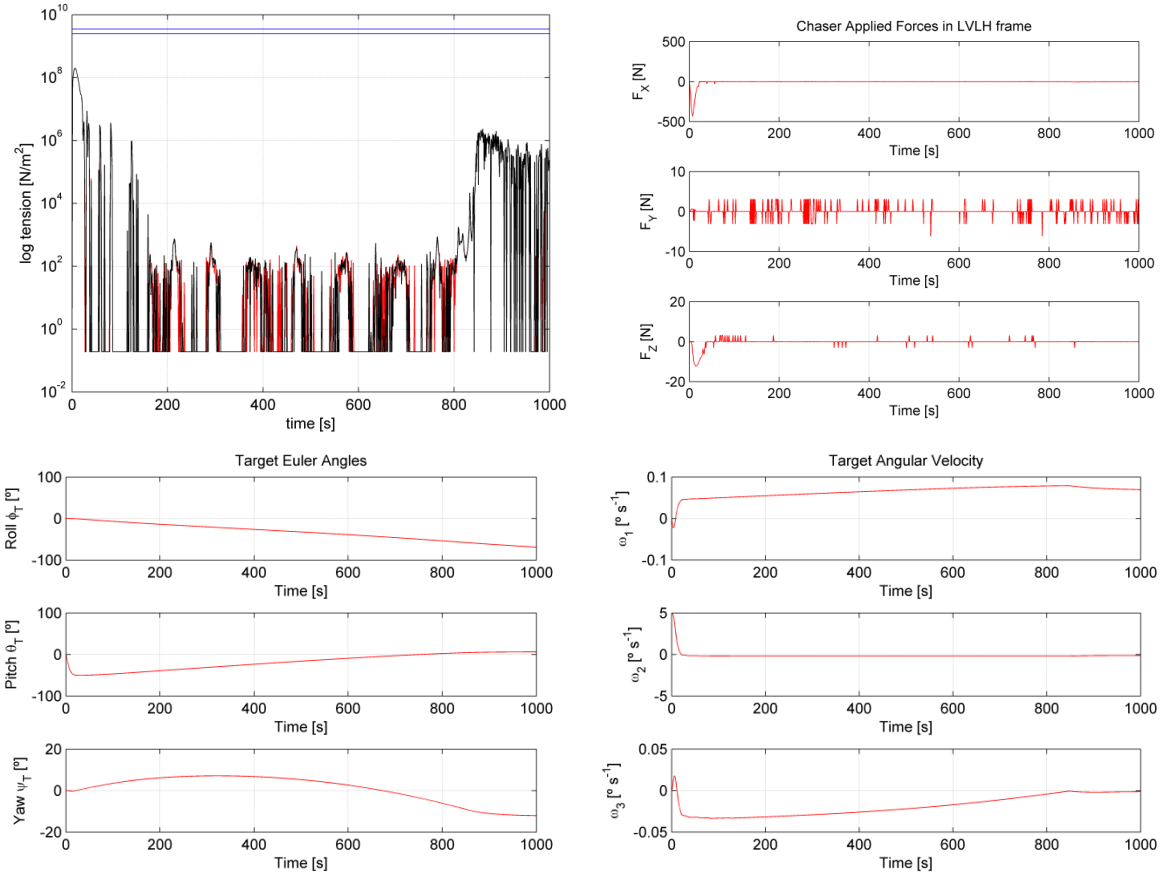


**Figure 6: (a) Tether tension, nominal case (b) ADR Chaser forces in LVLH frame, nominal case (c) Target attitude and (d) attitude rates, nominal case**

Figure 6b shows the chaser thruster forces in the LVLH frame. The maximum force during the initial stabilization is about 440 N, which is about half of the maximum allowable force (which is generated if all four 220 N assist thrusters are firing). Figures 6c and d show the attitude of the target and the attitude rates. The target starts with an angular velocity of 5 °/s, which is brought to zero within 20 s. The maximum deviation along the pitch axis is 50°.

### *2. De-orbit Burn*

For the de-orbit burn case, the initial rotation rate of the target is 0.5 °/s around the body y-axis. This value is lower than the 5 °/s at the start of the stabilization after capture case, considering that the target has been successfully stabilized during the maneuver. The length of the tether varies from 100 m to 400 m, and its stiffness varies from 100 N $m^{-1}$ to 2050 N $m^{-1}$. The burn maneuver starts after 10 seconds. After 10 seconds the target rotates away from its initial attitude that is perfectly aligned with the tether. The burn maneuver lasts 500 seconds and then a stabilization phase begins for 1000 seconds. The assist thrusters are active during the first 700 seconds after burning.

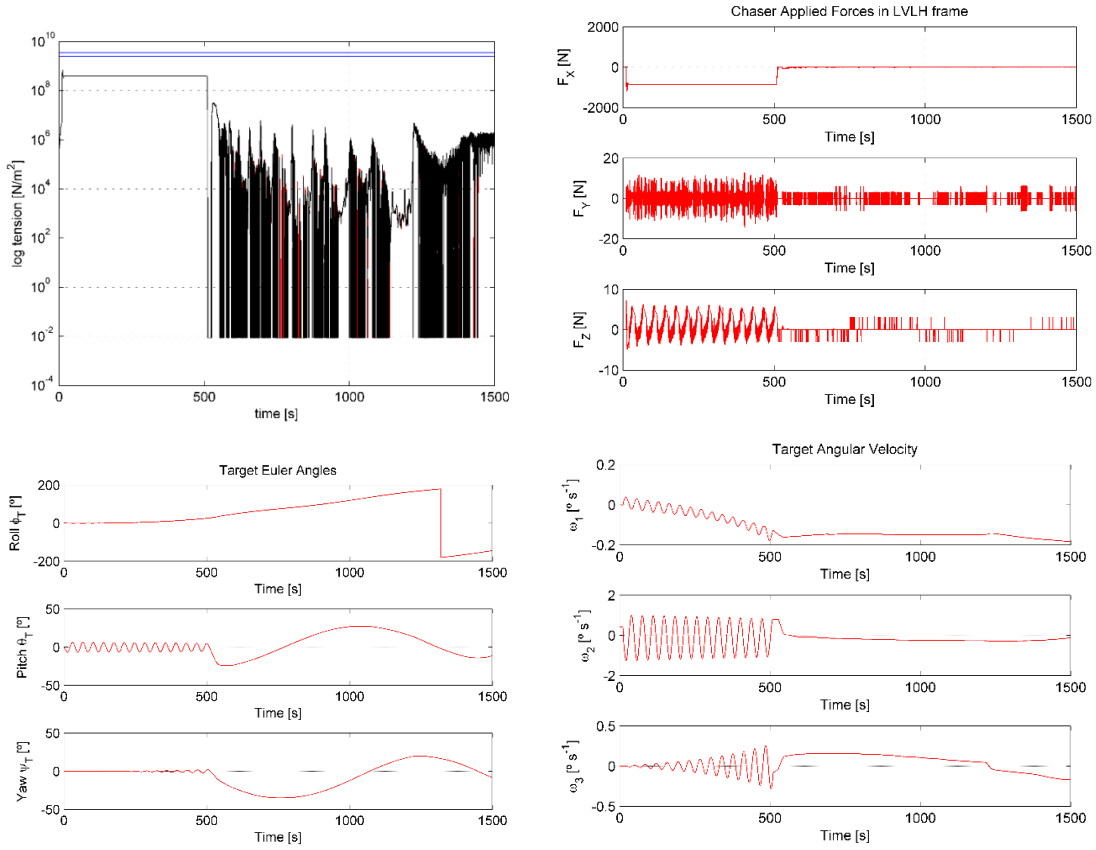


**Figure 7: (a) Tether tension (b) Chaser applied forces in LVLH frame - nominal case Target attitude and attitude rates, nominal case**

Figure 7a shows a slight overshoot at the beginning of the burn, followed by a constant tension profile until the end of the maneuver. Figure 7b shows the forces applied to the chaser for the nominal case. The tranquilization after the de-orbit burn shows a tension level similar to that of the tranquilization after the capture phase.

The ADR simulations indicate that proposed target capture/stabilization and de-orbit maneuvers are achievable with the proposed chaser/thruster architecture. The ADR mission reference scenario presented in this section is used to develop the ISS ADR experiments using free flyers to simulate the debris target and chaser, where the two free-flyers are connected with a tether to simulate the post capture/stabilization and de-orbit ADR maneuvers in a scaled but realistic manner.

## IV. ISS ADR Experiments using Free-flyers

Having defined the ADR reference mission scenario to scale for the ISS experiments, we examine the technical limitations and feasibility of the SPHERES free-flyers currently operated on the ISS for conducting ADR tests.

The SPHERES On-Board Software (OBSW) runs at a frequency of 10 Hz. SPHERES navigate by means of a combination of an inertial measurement system (consisting of 3 accelerometers and rate gyroscopes) and an ultrasound beacon system. The accuracy of the navigation solution that can be obtained is 1 mm in position and 1 mm/s in velocity. The angular rate is estimated with an accuracy of 0.4 °/s. It is important to note that 1 mm navigation accuracy on a tether length of 1 m for ISS ADR experiments implies an accuracy of 1 part in a thousand. This would correspond to a navigation accuracy of 0.1%, or 0.1 m accuracy for a tether of 100 m. This is equal or better than the performance of the true e.Deorbit sensors and navigation solution, which assumes an accuracy of 1% in range of the LIDAR sensor. Table 3 shows the mass properties of SPHERES.

| Parameter | Value |
|---|---|
| Mass [kg] | 4.4 |
| $I_{xx}$, $I_{yy}$, $I_{zz}$ [kgm$^2$] | 0.025, 0.023, 0.022 |
| $I_{xy}$, $I_{yz}$, $I_{zx}$ [kgm$^2$] | (0, 0, 0) |

**Table 3: SPHERES mass properties**

Figure 8a shows the layout of the thrusters. Each SPHERE carries 12 x 0.1 N cold gas thrusters, which together provide full 6 DOF control capability. Figure 8b shows the thruster firing sequence.

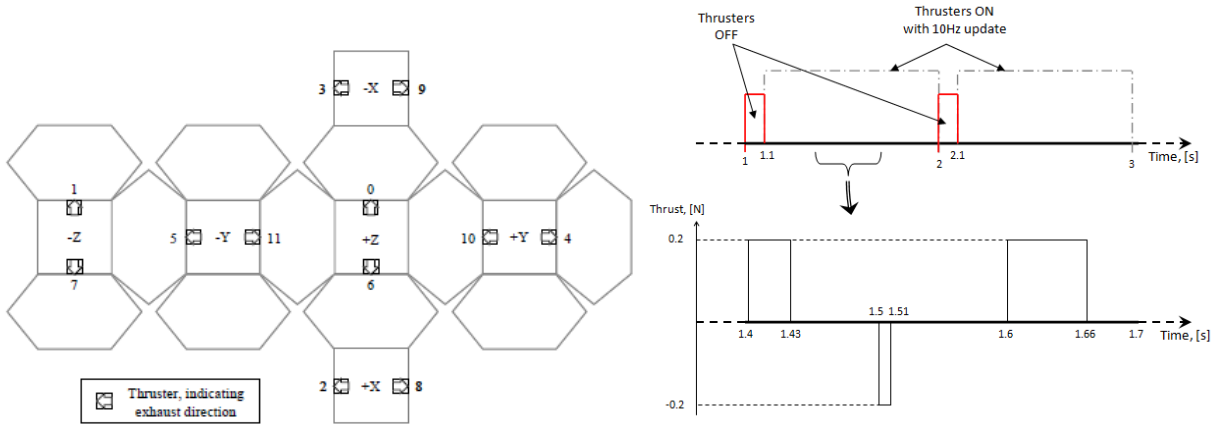


**Figure 8: (a) SPHERES thruster geometry (b) Assumed thrust ON-OFF cycle [19, 20]**

As stated in [18-21], the thrusters interfere with the ultrasound navigation. To ensure a reliable navigation solution all thrusters are turned off for 110 ms per second (see also [18]). These periods are referred to as 'thruster quiet time.' The minimum opening time of the thrusters is 10 ms. Figure 8b shows the firing pattern of a SPHERE. In this case, at every full second, a 110 ms period of thruster quiet time is inserted. During the rest of the second, the thrusters are updated at 10 Hz, with a minimum opening time of 10 ms. During each interval of 100 ms, a thruster can be fired for a duration ranging from 0 to 100 ms in steps of 10 ms. This leads to a thrust resolution of 0.01 N. The thruster geometry and firing pattern has been modelled into the SPHERES simulator used to perform ADR simulations in the following sections.

### A. Experimental Facility

The SPHERES experiments are proposed to take place in the Japanese/JAXA Pressurized Module (PM) 'KIBO' on the ISS. Kibo's Pressurized Module (PM) is a research facility where astronauts will enter and conduct scientific experiments or control Kibo's systems. The air composition inside the PM is nearly the same as that on earth. Figure 9 shows the specifications for the PM.

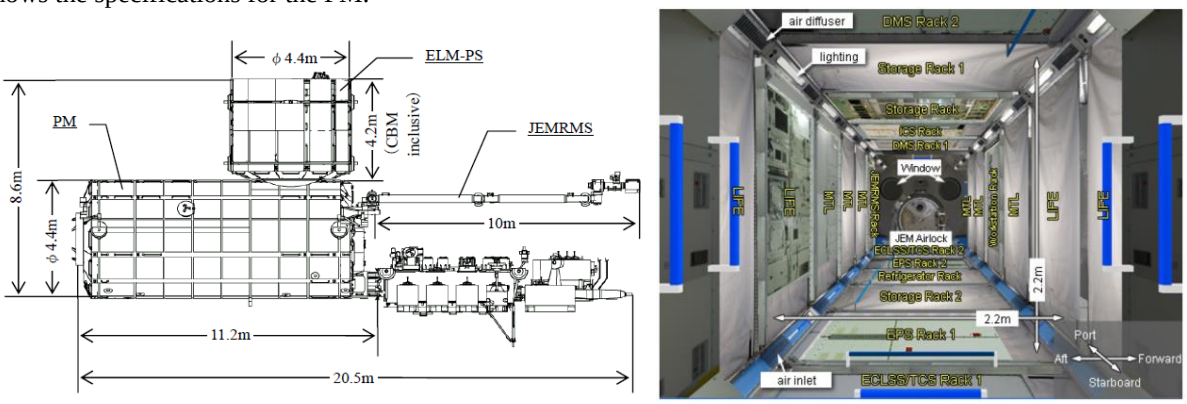


**Figure 9: ISS KIBO PM Dimensions and Internal Layout**

The KIBO PM module is one of the largest modules on ISS and the current volume set for SPHERES experiments is 2 $m^3$. However, it can be feasible to extend the volume available for ADR experiments for a short duration test campaign (hours) increase to 2 x 2 x 6 m (24 $m^3$).

### B. ADR Testing in the ISS

As already stated, the SPHERES experiments are proposed to take place in the Japanese 'KIBO' module on the ISS. The current available volume is 2 $m^3$ with the potential to increase to 2 m x 2 m x 6 m (24 $m^3$). Using a larger volume is preferable, since it allows for better fidelity of the analyzed scenario. To control the tension in the tether, the thrust will be fired at one direction for most of the time, since the corrections in the other axes (Y and Z axes) are performed less often. Therefore, the system will tend to move in one direction and using the whole length of the 'KIBO' module will be beneficial. Note that any experiment volume involving SPHERES is constrained by the position of the beacons allowing for the global position determination. When the limited space is of crucial importance, the tug SPHERE can be attached to the wall-mounted target SPHERE using a set of gimbals with active joints, see Figure 10. The target SPHERE can be given an initial attitude and angular rate with a very high level of precision and repeatability. One of the drawbacks of this set-up is the friction in the bearings, which can be mitigated with careful design.

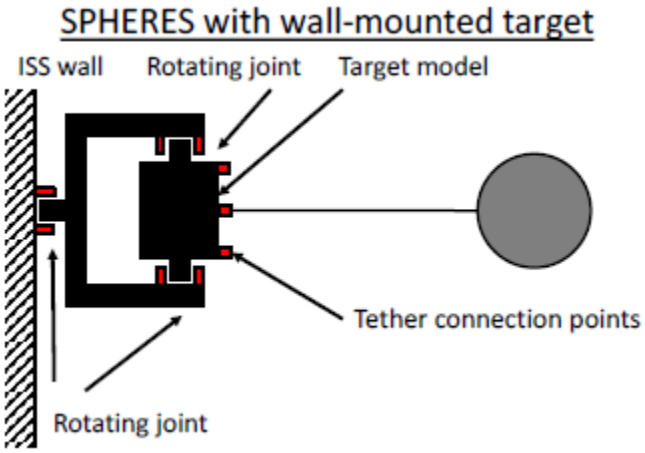


**Figure 10: SPHERES test setup for performing attitude stabilization tests**

To investigate the behavior of the system, the simulation was implemented using the developed software tool. In the simulation, initial attitude and angular rates of the tug and debris were assumed 0 in the ISS frame and initial tether elongation was equal 1%, which corresponds to 1 cm. Initially, a step input of 0.2 N was applied for 0.5 s and afterwards relative distance control and attitude stabilization were performed. This scenario can simulate the stabilization of the system after the main engine cut-off following the de-orbit burn. The test was run for 40 s. During the stabilization phase, the nominal thrust is 0.2 N, which results in the nominal force and torque equal 0.2 N and 0.02 Nm, respectively.

*1. Slack in the Tether*

Some 'worse case' scenarios for tether/ADR systems can be tested onboard the ISS using SPHERES to investigate the proposed design robustness. One of these undesirable behaviors is slack in the tether, which can be caused by the net slippage, shocks and other sources of disturbance. Using the simple PD controller implemented in the simulation tool, it is possible to recover from this scenario and to bring the tether back in tension. To investigate the behavior of the system, when the tether is in slack, the initial elongation was equal to -20% which corresponds to a 20 cm slack. Initial attitude and angular rates of the tug and debris were assumed 0 in ISS frame. From the start, the relative distance and attitude stabilization were performed. This scenario can simulate the stabilization of the system following the net slippage or some other source of the disturbance which causes the tether to go slack. The test was run for 40 s. During the stabilization phase, the nominal force and torque were kept the same as in the previous case, hence were equal 0.2 N and 0.02 Nm, respectively.

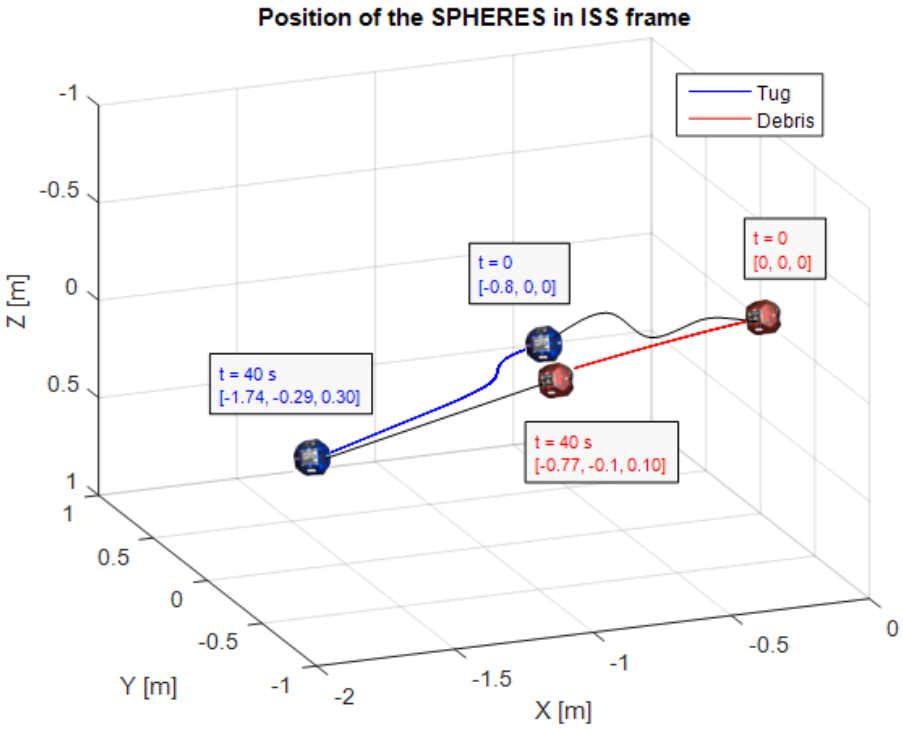


**Figure 11: SPHERES position in ISS frame, initial slack in the tether**

The position is represented in the ISS LVLH frame, assuming that the X axis is aligned with the longest dimension of the module and Z axis points downwards. It can be seen, that the system moves along the –X direction, the direction in which the initial 'de-orbit' burn was applied. During the 40s experiment, the most distant points are separated by 1.74 m, which is lower than in the previous case, when the tether was taut. This is due to the fact, that initially, when there is a slack in the tether, only the tug moves, since no force is applied to the target SPHERE. Position along the Y axis is greater and is equal to 0.3 m. Figure 12a presents the relative distance between the SPHERES, the tether tension and tether's angle from in-track direction. The tether tension is scaled by 140, i.e. the value read on the *right* axis, has to be divided by 140 to obtain the real tension. The system drifts towards +Z axis. Approximately, after 25 s, the tension in the tether is restored. Angular rates of the tug and debris are shown in Figure 12 (b). Greater oscillations of the debris can be explained by the pulls of the taut tether. Figure 12 (c) and (d) show the applied control force and torque. The control force is applied along the X-axis to bring back the tension in the tether.

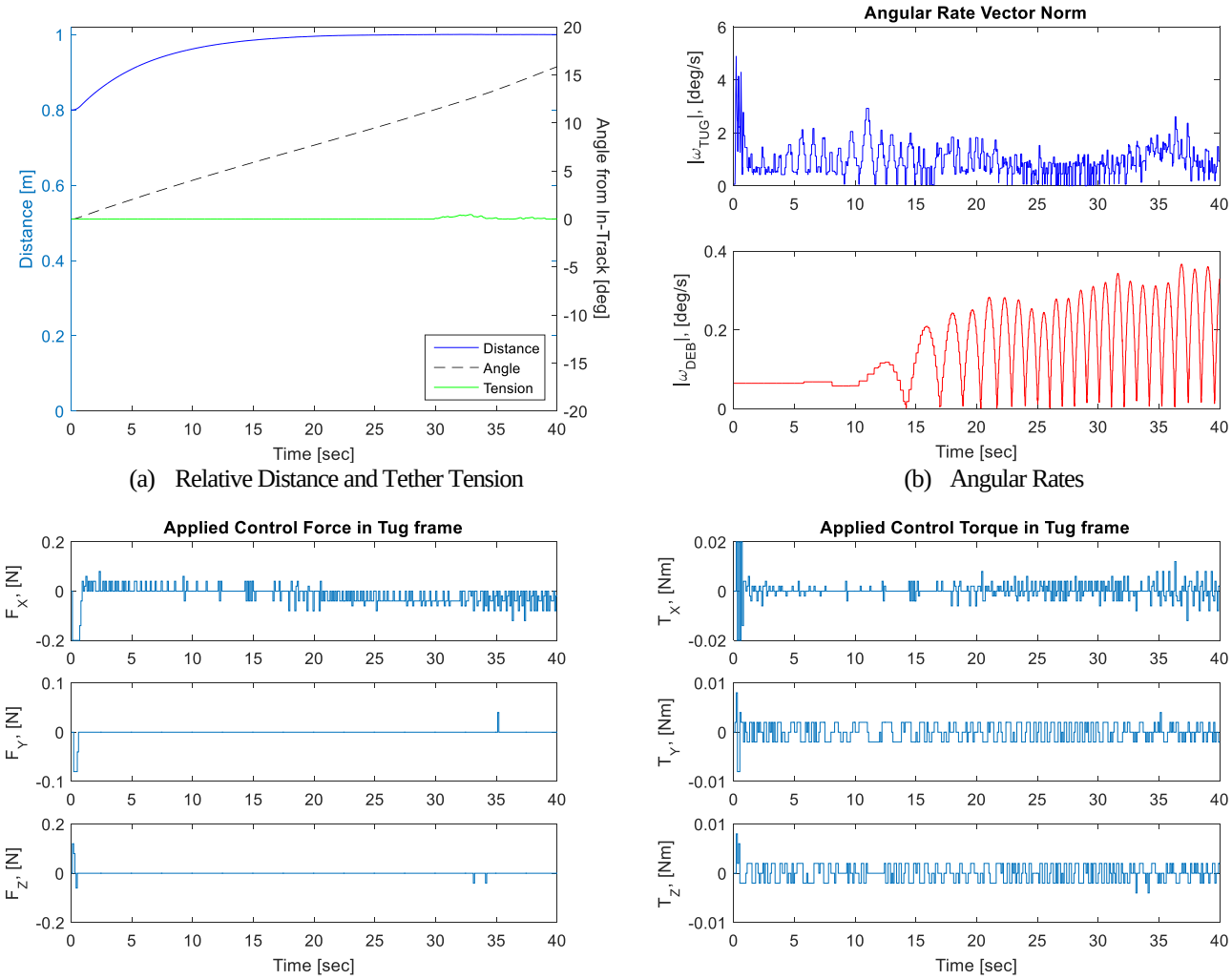


(a) Relative Distance and Tether Tension

(b) Angular Rates

(c) Applied Control Force

(d) Applied Control Torque

**Figure 12: Simulation parameters, slack in the tether**

This analysis shows, that a simple controller is able to stabilize the system in the presence of undesirable occurrences such as net slippage, shocks and other disturbances within the system. During the analysis, it was found, that the duration of the initial de-orbit burn does not influence the maximum chaser position along the X axis. This occurs as the most dominant cause for the drift along the –X axis is the applied thrust necessary to sustain the tension in the tether. Therefore, if decreasing the maximum X distance is critical, one can consider adjusting the thrusters feed pressure between 0 and 35 psig in the propulsion system of SPHERES. It is assumed, that the thrust decreases linearly with the feed pressure. Several simulations were implemented in order to investigate the maximum tug's position along the X axis. The torque was scaled accordingly, but the duration of the initial 'de-orbit' burn was kept equal 0.5 s. The results are presented in Table 4. Clearly, the maximum distance is well within the ISS KIBO volume available for experiments and confirms that ADR experiments on the ISS are feasible.

| Pressure [psig] | Pressure [kPa] | Thrust [N] | Maximum X distance [m] |
|---|---|---|---|
| 35 | 241.32 | 0.2 | -3.46 |
| 26.3 | 181.33 | 0.15 | -3.15 |
| 17.5 | 120.66 | 0.1 | -2.53 |
| 8.8 | 60.67 | 0.05 | -1.73 |
| 1.8 | 12.41 | 0.01 | -1.51 |

**Table 4: Maximum X-axis distance vs. SPHERES thruster pressure**

## V. ADR Simulations Using SPHERES

The simulation time for every scenario is 60 seconds, enough to stabilize the system. The tension level in the tether is well below the maximum through all the studied cases, so the results regarding those values have been omitted. The simulations start with an initial angular rate of 20 °/s. around the y-axis. Considering the added masses, the stored rotational kinetic energy is 2.1 mJ. As stated, the force applied to the target is 0.1 N, using the maximum 0.2 N force from the thrusters. However, the force is only applied during 90% of the time, as the first 10 ms of each second the thrusters are off. This effect has been added by multiplying the force applied to the target by 0.9 which leads to a maximum angle of 33°. For the 1m tether a nylon material is selected following a trade-off with soft rubber and rubber material options as it has shown to have a much better performance with respect to controllability and stiffness. The nylon 1m tether used in the simulation has a 1 mm diameter, a 0.79 $mm^2$ area and stiffness of 1571 N/m.

### A. Stabilization after capture

For the stabilization case, he initial elongation applied to the tether has been adjusted to conserve the initial potential and final kinetic energy throughout the first three cases. The energy has been adjusted to obtain a final relative velocity of 0.15 m/s after the conversion from potential to kinetic energy. The control gains on the controller have been adjusted to minimize the control effort. Every thruster activation adds energy to the system, which ultimately becomes kinetic energy of the two-mass system, increasing the travelled distance. For an ISS experiment, having a space constraint renders this as an important factor to take into account.

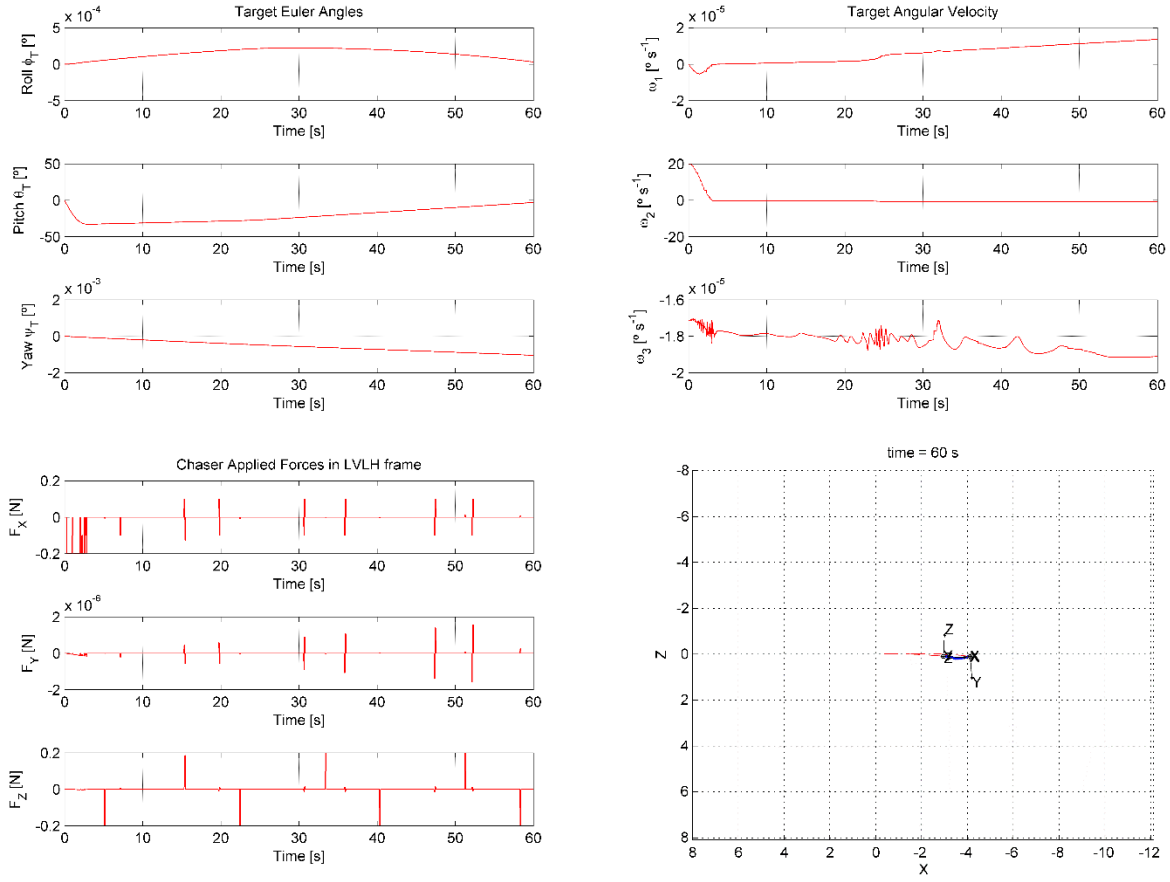


**Figure 13: (a) Target attitude (b) angular rate (c) Chaser applied forces in LVLH (d) Distance travelled by the spheres**

Figure 13a shows the maximum angle deviation from alignment. In this case, the peak value is 32.9 °. As it was mentioned, increasing the tether stiffness improves the control over the target. The target angular rate is reduced to 0.75 °/s at the end of the simulation. Figure 13c shows the forces applied to the chaser. The thrusters apply a force to stop the angular rate of the target for a similar amount of time, and then an opposite force to stop the motion. At the 15 seconds mark, the thrusters show a similar activity to control the rotation at the opposite point, as the angle has

changes from -32.9° to near 0°. Figure 13d shows that the distance travelled by the two spheres, reaching a maximum of 4.2 meters, which is compliant with the proposed ISS ADR experimental volume at the JEM module.

### B. De-orbit Burn

Figure 14a shows the stabilization of the position between the chaser and target (SPHERES free-flyers) after 35 seconds. The return distance in this case is 0.55 meters from the desired point. Figure 14b shows the distance travelled by the free-flyers. The required distance is 7.6 meters at the 60 second mark. Stopping the simulation at the 35 second mark, when the relative is fully stabilized, requires 4.9 meters. Figure 14c and d show the forces and torques applied to the chaser.

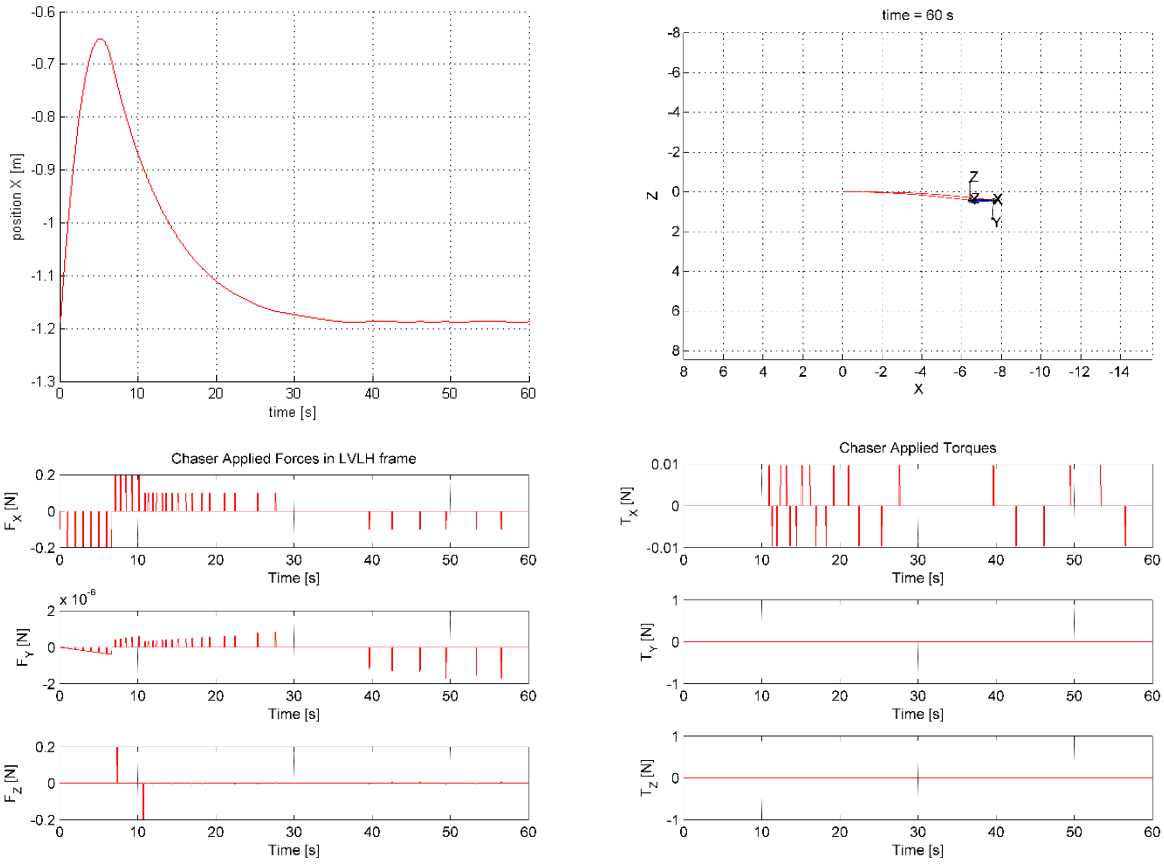


**Figure 14: (a) Relative from chaser to target (b) Distance travelled in ISS frame (c) Chaser applied forces (d) Chaser torques in LVLH frame**

### C. Stabilization during atmospheric pass

The behavior of the target during the e.Deorbit atmospheric pass could be simulated by using the target SPHERE's thrusters to provide forces and torques. An additional benefit of this approach would be that the target could provide a net force opposing the tether force, which would reduce the distance travelled with respect to the ISS during the experiment. The main problem with this approach is that the minimum accelerations (both linear and angular) that the thrusters can provide to SPHERES are at least an order of magnitude larger than the maximum accelerations that the drag force and torque can impart to Envisat. Table 5 shows a comparison between the accelerations imparted on Envisat by atmospheric drag and the accelerations imparted on SPHERES by means of the thrusters. The table shows that the accelerations differ by a factor of 10 – 100.

| Parameter | Envisat | SPHERES min | SPHERES max |
|---|---|---|---|
| **Mass [kg]** | 7800 | 4.4 | 4.4 |
| **Force [N]** | 2 | 0.2 | 0.02 |
| **Acceleration [m/s]** | 0.000256 | 0.045455 | 0.004545 |
| **M.O.I [kg·m$^2$]** | 125000 | 0.025 | 0.025 |
| **Arm [m]** | 12 | 0.11 | 0.11 |
| **Torque [Nm]** | 24 | 0.022 | 0.0022 |
| **Angular acceleration [rad/s]** | 0.000192 | 0.88 | 0.088 |

**Table 5: Comparison of Envisat drag accelerations to SPHERES thruster accelerations**

It therefore seems difficult to simulate the effect of atmospheric drag on the position and attitude of Envisat. It may still make sense to perform an experiment in which the target SPHERE is programmed to execute quasi-random force and torque maneuvers, simulating a fairly high level of disturbing torques. If the chaser GNC is able to cope with the level of perturbations that the target SPHERE can generate, then the true e.Deorbit GNC should certainly be able to cope with drag perturbations. Obviously, the time averaged force applied by the target SPHERE needs to be substantially lower than the maximum force that can be provided by the thruster. Otherwise, the chaser and the target would be capable of exerting equal force and torque and the chaser would not be able to control the target. For example, if the target fires its thrusters to approach the chaser at the same time as the chaser fires its thrusters to move away, then there would ideally be no net relative acceleration. This means that the chaser would not be able to drown out the disturbance force imparted by the target, which implies that the chaser does not have sufficient control authority. It is recommended to impart a force on the target of at most 0.02 N per clock cycle, that is, to operate the target thrusters at a maximum of 1/10$^{th}$ of the interval.

### D. Simulation Summary

The simulation results presented in this section confirm that ADR experiments for a chaser towing a target (debris), based on the ESA e.Deorbit reference study, using the SPHERES free-flyers are feasible and can bring useful insight on the GNC, mission planning and tether design of future ADR missions, at a low cost. The scaled parameters that have been selected are realistic: a tether with a length of 1 m made of rubber. This length ensures that the SPHERES remain inside the designated experiment volume of 2 x 2 x 6 m during each experiment of 60 seconds. Within these 60 seconds, a sufficiently large amount of the dynamical behavior of the system can be observed to draw conclusions on the behavior of the true system. It has been shown to be possible, to perform ADR experiments in a greatly reduced experiment volume by reducing the length of the tether substantially. A significant drawback of this reduced volume is that the body dimensions of the chaser and the target become more significant compared to the tether length. The body dimensions compared to tether length are already larger than in the e.Deorbit study if a tether length of 1 m is selected. It is therefore highly desirable to maintain an experiment volume of 2 x 2 x 6 m.

## VI. Proposed ADR-ISS Experiments

This section discusses the test scenarios to be proposed for implementation on the ISS, along with the required hardware and software configuration. Two main testing scenarios are proposed: (i) The initial stabilization. In this scenario, the target SPHERE is given an initial angular velocity that the chaser must nullify. (ii) The post de-orbit burn stabilization. In this scenario, the target and chaser SPHERE area released from a rig that can put the tether under tension, such that the de-orbit burn can be simulated. Three additional scenarios are variations of these two main scenarios: (i) Low-thrust de-orbit burns. In this scenario, the chaser SPHERE pulls the target SPHERE by means of its on-board thrusters at maximum feasible acceleration (ii) Tether tensioning between de-orbit burns. In this scenario, the chaser SPHERE puts a low level of tension in the tether to stabilize the configuration. The chaser SPHERE effectively pulls the target SPHERE, as in the previous scenario, but at a lower than maximum thrust (iii) Atmospheric pass. In this scenario, the target SPHERE provides disturbance forces and torques by means of its thrusters while the chaser attempts to stabilize the configuration.

## A. Hardware Configuration

*1. Extensometer*

The use of a tensiometer or an extensometer is envisaged in the e.Deorbit scenario. It would be highly desirable to include an extensometer to the experiment equipment. The SPHERES have a single port available for connecting an additional sensor, so it would be desirable to connect the extensometer to this input port. Alternatively, the extensometer data could simply be recorded for off-line analysis after the completion of the experiments.

*2. Tether material*

It is proposed that two to five different tethers will be tested. The tether length is set to 1 m. This length is a compromise between the space available and the proper scaling of the tether with respect to the e.Deorbit mission scenario. For the SPHERES tests a distance 6 m is available to perform the experiment, which means that the chaser and the target can move at most 4.58 m (that is, 6 m, minus the tether length, minus twice the diameter of a SPHERE). The scaling of the length units is as follows. In the case of e.Deorbit the length of the tether is 100 m and the distance of the tether attachment point to the center of mass is 5 m, such that the ratio of the distance of the tether attachment point to the center of mass to the length of the tether is 5%. For the SPHERES experiment, the distance of the tether attachment point to the center of mass is 0.11 m, such that in this case the ratio is 11%. This means that in the SPHERES experiment the chaser will be affected more by attitude motion of the target. The tether properties are examined in Table 6. Nylon and rubber are considered as tether materials. The last column provides the ranking of the tethers in order of priority for incorporation into the SPHERES experiments.

| material | D [mm] | A [mm$^2$] | E [GPa] | ρ [kg/m$^3$] | L [m] | k [N/m] | m [g] | m / m-SPHERE [%] | # |
|---|---|---|---|---|---|---|---|---|---|
| rubber (soft) | 1 | 0.79 | 0.01 | 1000 | 1 | 7.8 | 0.79 | 0.18 | |
| rubber (soft) | 2 | 3.14 | 0.01 | 1000 | 1 | 31.4 | 3.14 | 0.71 | 5 |
| rubber (soft) | 3 | 7.07 | 0.01 | 1000 | 1 | 70.6 | 7.07 | 1.61 | |
| rubber | 1 | 0.79 | 0.1 | 1100 | 1 | 78.5 | 0.86 | 0.20 | 2 |
| rubber (soft) | 4 | 12.57 | 0.01 | 1000 | 1 | 125.6 | 12.57 | 2.86 | |
| rubber | 2 | 3.14 | 0.1 | 1100 | 1 | 314.1 | 3.46 | 0.79 | 3 |
| rubber | 3 | 7.07 | 0.1 | 1100 | 1 | 706.8 | 7.78 | 1.77 | |
| rubber + nylon | 1 | 0.79 | 1 | 1100 | 1 | 785.4 | 0.86 | 0.20 | 1 |
| rubber | 4 | 12.57 | 0.1 | 1100 | 1 | 1256.6 | 13.82 | 3.14 | |
| nylon | 1 | 0.79 | 2.4 | 1140 | 1 | 1884.9 | 0.90 | 0.20 | 4 |

**Table 6: Tether materials and properties**

The tethers that are ranked 1 and 2 span an order of magnitude in stiffness. Tether 3 provides an additional sample in between tethers 1 and 2. Tether 4 is somewhat stiffer and compares well to the higher stiffness designs proposed by industry. Tether 5 has a very low stiffness.

## B. Software configuration

For each scenario, the navigation function that is currently present in SPHERES will be used. The accuracy of the navigation is 1 mm in position. As noted earlier, 1 mm navigation accuracy on a tether length of 1 m implies an accuracy of 1 part in a thousand. This would correspond to a navigation accuracy of 0.1%, or 0.1 m accuracy at 100 m. This accuracy should be sufficient to perform all tether experiments. If possible the measurements from the extensometer should be made available to the OBSW. It is expected that a separate navigation filter should treat the output from the extensometer. The information from the extensometer needs to be made available to the guidance/ control functions. Alternatively, the current elongation of and tension in the tether needs to be estimated based on the relative position and attitude of the chaser SPHERE with respect to the target SPHERE.

*1. Experiment duration and stop distance*

The nominal duration for each experiment is 60 seconds. Simulations show that in most cases during this period the dynamics exhibit both the transient associated with stabilization and the onset of steady state behavior. Furthermore, at around 60 seconds, the chaser-target system runs the risk to collide with the edge of the experiment volume. For

each scenario, both the target and the chaser SPHERE are envisaged to be equipped with a guidance function that can terminate the experiment when the chaser reaches a certain distance from the edge of the experiment volume with a velocity that the SPHERE can stop when performing a maneuver at full thrust. At full thrust (assuming still the thruster quiet time of 110 ms per second) a SPHERE can achieve an acceleration of about 4 cm/s

*2. Control update frequency*

The control command update frequency can be lowered to 1 Hz. This is an option that could be added as an optional feature to each of the test scenarios discussed below.

### C. Thruster force implications

It is envisaged that the e.Deorbit mission be performed with a chaser spacecraft that features three distinct sets o thrusters. The de-orbiting will be performed by means of two (or four) 425 N thrusters, helped by four assist thrusters of 220 N that can operate in pulse mode. Twenty-four 22 N RCS thrusters are used to control the relative position and attitude of the chaser. This means that in the direction of the tether force the e.Deorbit chaser can apply control force very precisely and in a broad range of force ranging from 0 to 880 N.

The SPHERES have only a single type of thruster that generates a thrust of 0.1 N. The pulse modulation scheme used causes the thrust to be available in discrete steps of 0.01 N. The e.Deorbit scenario can be scaled to the SPHERES system in two ways: either the system is scaled such that the SPHERES thrusters mimic the behavior of e.Deorbit using the 220 N thrusters, or the system can be scaled such that they mimic e.Deorbit using the 22 N thrusters. If the system is scaled for one of the two, then the other cannot be effectively simulated due to the limitations imposed by the SPHERES thrusters. This implies that the de-orbit burn cannot be effectively simulated using the SPHERES thrusters. In e.Deorbit, the main thrusters would be on continuously during the de-orbit burn. Position and attitude control would be performed by means of the 220 N assist thrusters and the 22 N RCS thrusters. SPHERES has only a single type of thruster, and if a quasi-continuous force is provided to put tension in the tether, then this means that certain thrusters need to be on all the time (except during the thruster quiet time used for navigation). This in turn limits the availability of control force and torque in certain directions, because the thrusters used for tensioning cannot be used. Summarizing, there are two important limitations to the simulation of the de-orbit burn: the scalability of the thrust level, and the restriction of control authority if the chaser SPHERE thrusters are used to perform the de-orbit burn. Several work-arounds are possible: (i) Use of a rig to tension the tether. In this case, the de-orbit burn itself is not simulated; only the release of tension after the de-orbiting thrusters are switched off. The stabilization after the burn can be studied. The thrusters are scaled to behave as the RCS thrusters and the restriction of control authority is avoided. (ii) Reduction of representativeness. In this case, a simple 'pull' experiment is performed where one SPHERE pulls the other. This would simulate a scenario where the RCS thrusters are used to de-orbit Envisat, i.e., it is not a realistic scenario. On the other hand, an experiment like this one could be used to determine what level of tension is appropriate in between the de-orbit burns to maintain a stable configuration. Also, no additional hardware is required. (iii) Use of time-sharing of the chaser thrusters. In this case, the SPHERES thrusters are alternately used to simulate the de-orbit burn during one step of the OBSW and used to perform control during the next. It is not expected that this will lead to good results, because the de-orbiting thrusters will not be always on and because this strategy reduces the thrust level available for the simulated de-orbit burn even further. (iv) Use of the target SPHERE thrusters to tension the tether. In this case, the relevant target SPHERE thrusters are set to always on (except for the thruster quiet time), and the chaser performs the control. The representativeness of such an experiment is doubtful, because the attitude of the target would be determined by other factors apart from the tether itself.

### *D. Experimental Set-up*

*1. Target Attitude Stabilization*

In the attitude stabilization test scenario, the target SPHERE is spun up using its own thrusters. When the target reaches the desired angular velocity of about 20 °/s, the chaser SPHERE performs maneuvers to stop the attitude motion of the target and stabilize its attitude. This scenario is representative of the e.Deorbit stabilization immediately after capture. In a free-floating experiment the hardware configuration consists of the chaser and the target SPHERE connected by means of a 1 m tether. Simulations indicate that the initial stabilization can be performed within the 6 m that are available in the ISS.

Attitude motion during the stabilization phase could also be studied in a wall-mounted configuration using a universal / Cardan joint with low friction. Figure 10 shows an illustration of the set-up proposed. The advantage of such a setup is that it allows for more time to perform the experiment. That is, if the experiment is free-floating, then the entire

system will accelerate whenever the chaser issues a control pulse. The free-floating experiment duration is then limited by the size of the space station module. A wall-mounted rig would not have this problem. Another advantage is that if the joints are active, then the target could be given any initial attitude and any initial attitude rate with great precision and repeatability, allowing for multiple experiments with highly similar initial conditions. The major disadvantage is that the bearings of the joint would introduce friction into the system such that the attitude dynamics would differ from free-floating dynamics.

*2. Post de-orbit burn stabilization*

This experiment simulates the stabilization after the de-orbit burn. More specifically, it simulates the stabilization of the target and chaser attitudes and the relative position as the tether tension is released following main engine thrust cutoff. The primary objective of this test would be to demonstrate the capability to stabilize the relative position of the chaser with respect to the target after a simulated de-orbit burn. Secondary objectives can include: (i) Assess the impact of the tether stiffness on the stabilization of the relative position after a simulated de-orbit burn (ii) Assess the impact of different controllers (i.e., both parameters and controller structure) on the attitude stabilization (iii) Assess the impact of changing the control update frequency to 1 Hz. The post-burn stabilization requires a rig to tension the tether because of the limitations of the thrusters discussed in section III. Free floating tests would be more representative, but cannot be realistically performed using the SPHERES thruster configuration. Figure 15 shows several ideas on how to construct a rig for setting up the tethered de-orbiting experiments.

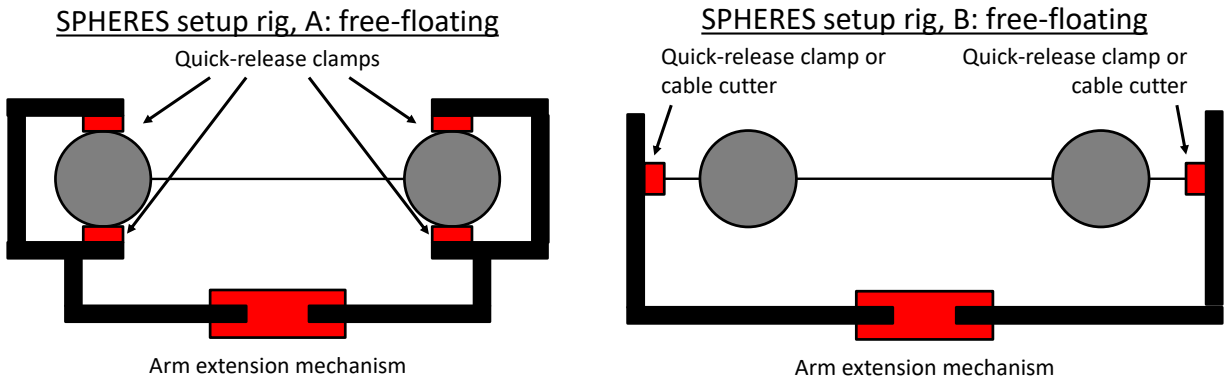


**Figure 15: SPHERES setup rig options**

The rig will feature an arm with adjustable length, such that the level of tension in the tether can be controlled. The release mechanism could be implemented as quick-release clamps or as a cable that can be cut. In the former case, the mechanism could conceivably also impart attitude motion to one of the two SPHERES, and the initial spin-up of target could be used to simulate stabilization phase. In the latter case, the disturbance forces and torques imparted by the release mechanism onto the SPHERES is smaller, such that the dynamics are represented more closely. Normally, the rig would be stationary with respect to the ISS. However, in case of a free-floating rig, the entire rig could be given an initial velocity before release. This would allow a longer duration of the experiment. The rig would be given an initial velocity towards the right, such that at the start of the experiment, both SPHERES are at the left of the module, moving towards the right with equal velocity. The SPHERE on the left starts pulling the SPHERE on the right, slowing it down, and eventually pulling it back towards the left. In this way the use of space can be maximized.

*3. Low-thrust de-orbit burns*

This experiment simulates the de-orbit burn itself, as if it were performed with thrusters with a fairly low force. Due to the limited resolution of the thrust level of SPHERES (see section III), this experiment is not fully representative of the e.Deorbit de-orbit burn. The primary objective of this experiment would be to (i) demonstrate the capability to accelerate a target by means of a tethered connection (ii) Demonstrate the capability to stabilize the relative position and attitude of the chaser with respect to the target during a de-orbit burn. An alternative option is to attach a single SPHERE directly to the wall of the ISS. The SPHERE would then perform a simulated de-orbit burn. In this case only the second test objective can be addressed. To establish initial conditions, a rig could be used. A diagram of such a rig is shown in Figure 16. This rig could also be used to pre-tension the tether prior to release.

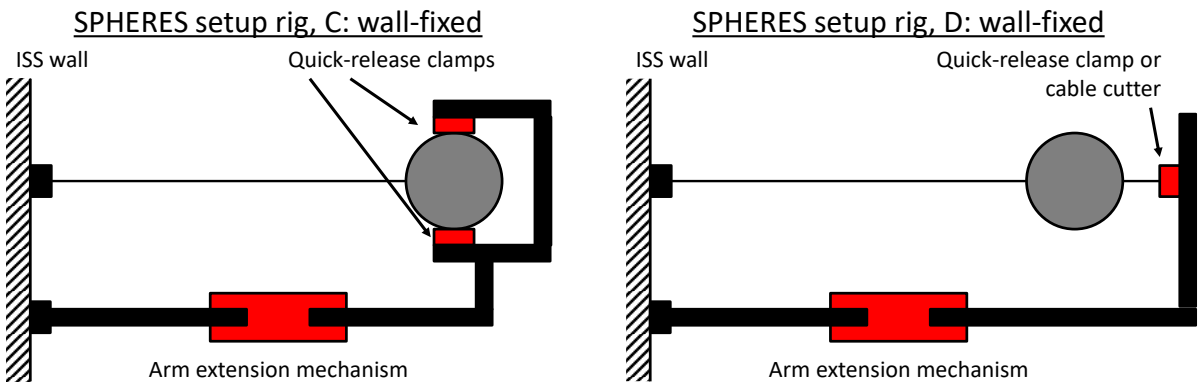


**Figure 16: SPHERES wall mounted rig options**

*4. Tether tensioning between de-orbit burns*

This experiment aims to determine the level of tension required in the tether to maintain a stable configuration of the chaser, target and tether. A small random attitude rate is provided to the target at the start of the experiment. The primary objective is to determine the level of tension required to maintain the chaser, target and tether in a stable configuration. Implementation of this test would involve two SPHERES free-flyers connected by means of a tether with a length of 1 m. The set-up of Figure 15 will be used in this experiment.

*5. Atmospheric pass*

In this experiment, the level of tension required in the tether to maintain a stable configuration of the chaser, target and tether in conditions that are similar to the atmospheric pass will be investigated. The target provides disturbing forces and torques during the experiment.

## VII. Conclusion

In this paper, it has been shown that it is feasible to perform low cost, scaled experiments in the ISS using SPHERES which can provide useful information on tethered de-orbiting of Envisat and other large mass space debris objects. Two main testing scenarios have been investigated. Realistic ADR test scenarios have been developed in experiments, that last 60 seconds at most, such as for the initial stabilization after capture and post de-orbit burn stabilization phases of a realistic ADR reference mission such as e.Deorbit. The tether parameters have significant influence on the attitude motion of the target. Careful tether design reduces the risk of the target rotation excitation even when the step deorbit burn is performed. A simple rig to be used on the ISS with the SPHERES free-flyers is proposed to simulate the de-orbit burn, because of the limitations of the SPHERES thrusters. Low-thrust de-orbit scenarios can be simulated without the use of a rig, although the SPHERES thrusters that simulate the de-orbit thrusters will need to be used to control the chaser-target configuration as well. Although it is possible to perform experiments within a reduced volume of 2 $m^3$ and a shorter tether, it is strongly recommended to use a larger volume of 2 x 2 x 6 m and a longer tether of 1 m length. Simulations show that having a single axis large dimension of 6 m is crucial for performing the experiments with a 1 m long tether. Various additional useful experiments have been analyzed such as the testing of to five different tethers with different stiffness and each having a length of 1 m. In addition, it is proposed to test different versions of the on-board software, specifically, to test different guidance and control functions, and different control command update frequencies. In this paper, it has been shown that low cost, novel scaled ADR experiments can be conducted on the ISS using the SPHERES free-flyer which can take place in a very short time, use existing infrastructure with very little add-on hardware required. The proposed experiments have shown that crucial insight can be gained on the tether properties, dynamics and control behavior of tether end bodies which can be used for future ADR missions.

### Acknowledgements

The work presented was funded by the European Space Agency under contract No. 4000116843/16/NL/GLC

## References

[1] Beletsky, V. V., and Levin, E. M., *Dynamics of Space Tether Systems*, *Advances in the Astronautical Sciences*, Vol. 83, American Astronautical Society Publications, San Diego, CA, 1993, pp. 20-33.

[2] Kessler, D. J., Johnson, N. L., Liou, J. C., and Matney, M., "The Kessler Syndrome: Implications to Future Space Operations," *33rd Annual AAS Guidance and Control Conference*, AAS Paper 2010-016, Breckenridge, CO, Feb. 2010.
[3] Liou, J. C., "An Active Debris Removal Parametric Study for LEO Environment Remediation," *Advances in Space Research*, Vol. 47, No. 11, 2011, pp. 1865-1876, doi: 10.1016/j.asr.2011.02.003
[4] Reed, J., and Barraclough, S., "Development of Harpoon System for Capturing Space Debris," *6th European Conference on Space Debris*, ESA SP-723, Darmstadt, Germany, April 22 – 25, 2013.
[5] Retat, I., Bischof, B., Starke, J., Froth, W., and Bennell, K., "Net Capture System," *2nd European Workshop on Active Debris Removal*, Paper No. 4.3, Quentin, Paris, June 18 – 19 2012.
[6] Reed, J., Busquets, J., and White, C., "Grappling System for Capturing Heavy Space Debris," *2nd European Workshop on Active Debris Removal*, Paper No. 4.2, Quentin, Paris, June 18 – 19, 2012.
[7] Nishida, S., and Yoshikawa, T., "Space Debris Capture by a Joint Compliance Controlled Robot," *Proceedings of the 2003 IEEE/ASME International Conference on Advanced Intelligent Mechatronics (AIM 2003)*, Vol. 1, Kobe, Japan, July 20 – 24, 2003, pp. 496-502, doi: 10.1109/AIM.2003.1225145
[8] Jasper, L., Schaub, H., Seubert, C., Valery, T., and Yutkin, E., "Tethered Tug for Large Low Earth Orbit Debris Removal," *AAS/AIAA Astrodynamics Specialists Conference*, Paper No. AAS 12-252, Charleston, SC, January 29 – February 2, 2012.
[9] Jasper, L., and Schaub, H., "Input Shaped Large Thrust Maneuver with a Tethered Debris Object," *Acta Astronautica*, Vol. 96, March-April 2014, pp. 128-137, doi: 10.1016/j.actaastro.2013.11.005
[10]Jasper, L., and Schaub, H., "Tether Design Considerations for Large Thrust Debris De-Orbit Burns," *AAS/AIAA Space Flight Mechanics Meeting*, Paper No. AAS 14-443, Santa Fe, NM, January 26 – 30, 2014.
[11] Jasper, L., and Schaub, H., "Tethered Towing Using Open-Loop Input-Shaping and Discrete Thrust Levels," *Acta Astronautica*, Vol. 105, No. 1, Dec. 2014, pp. 373-384, doi: 10.1016/j.actaastro.2014.10.001
[12] Jasper, L., "Open-Loop Thrust Profile Development for Tethered Towing of Large Space Objects," Ph.D. Thesis, Aerospace Engineering Sciences Dept., Univ. of Colorado, Boulder, CO, 2014.
[13] Linskens, H. T. K., and Mooij, E., "Tether Dynamics Analysis and Guidance and Control Design for Active Space-Debris Removal," *Journal of Guidance, Control and Dynamics*, Vol. 39, No. 6, 2016, pp. 1232-1243. doi: 10.2514/1.G001651
[14] Aslanov, V. S., and Yudintsev, V. V., "Dynamics of Large Space Debris Connected to Space Tug by a Tether," *Journal of Guidance, Control and Dynamics*, Vol. 36, No. 6, 2013, pp. 1654-1660, doi: 10.2514/1.60976
[15] Aslanov, V. S., and Yudintsev, V. V., "Dynamics of Large Space Debris Removal Using Tethered Space Tug," *Acta Astronautica*, Vol. 91, Oct.-Nov. 2013, pp. 149-156, doi: 10.1016/j.actaastro.2013.05.020
[16] Aslanov, V. S., and Ledkov, A. S., "Dynamics of Towed Large Space Debris Taking Into Account Atmospheric Disturbance," *Acta Mechanica*, Vol. 225, No. 9, 2014, pp. 2685-2697, doi: 10.1007/s00707-014-1094-4.
[17] Biesbroek, R., Hüsing, J., and Wolahan, A., "System and Concurrent Engineering for the eDeorbit Mission Assessment Studies," *6th International Systems and Concurrent Engineering for Space Applications Conference*, Stuttgart, Germany, Oct. 2014.
[18] Mohan, S, Saenz-Otero, A, Nolet, S, Miller, D W, Sell, S, 'SPHERES flight operations testing and execution', *Acta Astronautica (2009), doi: 10.1016/j.actaastro.2009.03.039*
[19] Chung S, Miller D. (2007) 'Nonlinear Control and Synchronisation of Multiple Lagrangian Systems with Application to Tethered Formation Flight Spacecraft', PhD Thesis, MIT
[20] Nolet, S., Saenz-Otero, A., Miller, D. W., and Fejzic, A., "SPHERES Operations Aboard the ISS: Maturation of GN&C Algorithms in Microgravity," 30th Annual AAS Guidance and Control Conference, No. AAS 07-042, Breckenridge, Colorado, 2007.
[21] Pong, C M, Saenz-Otero, A, Miller D W, 'Autonomous Thruster Failure Recovery on Underactuated Spacecraft using Model Predictive Control', AAS Guidance and Control Conference, Breckenridge, CO, Paper #11-033, 2011
[22] Bualat, M., Barlow, J., Fong, T., Provencher, C., Smith, Trey, Zuniga, A., 'Astrobee: Developing a Free-flying Robot for the International Space Station', AIAA SPACE 2015 Conference and Exposition, SPACE Conferences and Exposition, (AIAA 2015-4643).
[23] Biesbroek, J. R. 'Introduction to e.DEORBIT', ESA Cleanspace workshop, 2016, Link: https://indico.esa.int/indico/event/128/material/2/0.pdf, Accessed June 1, 2016
[24] J. Telaar, 'e.Deorbit Phase B1 GNC and Combined Control, Simulation Results', ESA Cleanspace workshop, 2016, https://indico.esa.int/indico/event/128/material/5/7.pdf, Accessed June 1, 2016
[25] Falcoz, A. Moro , V., 2014, "AGADiR - Advanced GNC for Active Debris Removal," e.Deorbit Symposium, 2014 – Noordwijkerhout, The Netherlands

[26] Lappas VJ, Forshaw JL, Pisseloup A, Salmon T, Joffre E, Chabot T, Retat I, Axthelm R, Barraclough S, Ratcliffe A, Bradford A, Kadhem H, Navarathinam N, Rotteveel J, Bernal C, Chaumette F, Pollini A, Steyn WH. (2014) 'RemoveDEBRIS: An EU Low Cost Demonstration Mission to Test ADR Technologies'. Toronto: 65th International Astronautical Congress

[27] Kucharski, D., Kirchner, G., Koidl, F., Fan, C., Carman, R., Moore, C., et al., "Attitude and Spin Period of Space Debris Envisat Measured by Satellite Laser Ranging," *IEEE Transactions on Geoscience and Remote Sensing*, Vol. 52, No. 12, Dec. 2014, pp. 7651-7657, doi: 10.1109/TGRS.2014.2316138

[28] CDF, "e.deorbit CDF study report CDF", CDF-135(C) , Sep 2012

[29] B. Bastida Virgili, S. Lemmens, H. Krag, Investigation on Envisat attitude motion, e.Deorbit Workshop, 2014

[30] Airbus Defence and Space, "Space Propulsion - Chemical Bi-Propellant Thruster Family 4N, 10N, 22N, 200N, 400N", Data Sheet, 2013

[31] F. Zhang and P. Huang, "Releasing Dynamics and Stability Control of Maneuverable Tethered Space Net," in *IEEE/ASME Transactions on Mechatronics*, vol. 22, no. 2, pp. 983-993, April 2017. doi: 10.1109/TMECH.2016.2628052

[32] Huang, P., Wang, D., Zhang, F., Meng, Z., and Liu, Z., 'Postcapture robust nonlinear control for tethered space robot with constraints on actuator and velocity of space tether'. International Journal of Robust Nonlinear Control, 27: 2824–284, 2017. doi: 10.1002/rnc.3712.

[33] Minghe Shan, Jian Guo, Eberhard Gill, 'Contact dynamic models of space debris capturing using a net', Acta Astronautica, 2017, ISSN 0094-5765, https://doi.org/10.1016/j.actaastro.2017.12.009

[34] Yakun Zhao, Panfeng Huang, Fan Zhang, 'Dynamic modeling and Super-Twisting Sliding Mode Control for Tethered Space Robot', Acta Astronautica, Volume 143, 2018, Pages 310-321, ISSN 0094-5765, https://doi.org/10.1016/j.actaastro.2017.11.025

[35] Bingheng Wang, Zhongjie Meng, Panfeng Huang, Attitude control of towed space debris using only tether, Acta Astronautica, Volume 138, 2017, Pages 152-167, ISSN 0094-5765, https://doi.org/10.1016/j.actaastro.2017.05.012

[36] Jingrui Zhang, Keying Yang, Rui Qi, 'Dynamics and offset control of tethered space-tug system', Acta Astronautica, Volume 142, 2018, Pages 232-252, ISSN 0094-5765, https://doi.org/10.1016/j.actaastro.2017.10.020

[37] P. Huang, F. Zhang, J. Cai, D. Wang, Z. Meng and J. Guo, "Dexterous Tethered Space Robot: Design, Measurement, Control, and Experiment," in *IEEE Transactions on Aerospace and Electronic Systems*, vol. 53, no. 3, pp. 1452-1468, June 2017, doi: 10.1109/TAES.2017.2671558